Physica C 192 (1992) 481–490
North-Holland

PHYSICA C

Dependence of T_c on the oxygen distribution in the Cu–O chains in the high temperature superconductors $YBa_2Cu_3O_{6+x}$

G.V. Uimin [a], V.F. Gantmakher [b], A.M. Neminsky [b], L.A. Novomlinsky [b], D.V. Shovkun [b] and P. Brüll [b,c]

[a] *Landau Institute for Theoretical Physics, ul. Kosygina 2, Moscow 117940, Russia*
[b] *Institute of Solid State Physics, Chernogolovka 142432, Moscow District, Russia*
[c] *Universität Konstanz, W-7750 Konstanz 1, Germany*

Received 5 January 1992

It is experimentally confirmed that in $YBa_2Cu_3O_{6+x}$ ceramics with x fixed within the range 0.4–0.5 the temperature of the superconducting transition T_c can be appreciably reduced by quenching a sample from moderate temperatures between 50°C and 200°C. The theory developed for the description of the ensemble of Cu–O– ... chain fragments in orthorhombic phase is applied for the explanation of the experimental results, which can be interpreted as follows. In ortho-II phase the oxygen filling factors in oxygen deficient Cu(1) planes alternate from row to row. Alternation decreases with temperature increasing. Redistribution of the oxygen ions between the rows increases the fraction of short Cu–O– ... chain fragments which cannot inject holes into CuO_2 planes. This diminishes the hole concentration in the Cu(2) planes and, hence, T_c. Near 150°C the sample undergoes the second order transition into ortho-I phase where rows are equally filled with oxygen. Further increasing of the temperature does not reveal an appreciable reduction of T_c. A comparison of the experiment with the simplest model is performed.

1. Introduction

The superconducting properties of the CuO-based high temperature superconductor $YBa_2Cu_3O_{6+x}$ (YBCO) are strongly affected by variation of the oxygen content. When x changes from 1 to ≈ 0.4 the transition temperature T_c decreases, leading finally to the complete vanishing of superconductivity. The variations in the oxygen content result in filling the oxygen vacancies in Cu(1) chains, which are responsible for the carrier doping to the CuO_2 (Cu(2)) planes. On changing x from ≈ 0.55 to ≈ 0.7 the transition temperature increases insignificantly, displaying a plateau-like behavior of T_c versus x. In the region around $x \approx 0.5$ the ortho-II phase has been identified which corresponds to the double-cell structure with alternation of oxygen-rich and oxygen-poor chains within the Cu(1) plane [1–3].

Recently the experiments with quenched YBCO single crystals have been reported in which a decrease of the transition temperature without changing the oxygen stoichiometry had been observed [4,5]. This means that not only the oxygen content but also the distribution of oxygen ions within the chains can influence the transition temperature T_c. The relevant quenching temperature range between ≈ 300 K and 450 K appears to be rather narrow. This circumstance should be a guide while analysing a possible explanation of the phenomenon which exhibits intriguing correspondence between the oxygen content x, the transition temperature T_c, the quenching temperature T_q and the density of carriers in Cu(2) planes. There is a prerequisite we need in order to reveal the mechanism of ortho-I–ortho-II phase transition. The goal of this paper comprising both experimental measurements and their theoretical interpretation is to realize unambiguously the role of chains in YBCO and related topics.

The paper is organized as follows.

In the following section we present the experimental results which were obtained on YBCO ceramics. In essence, they are in agreement with the results for single crystals [4]: if the initial transition temperature T_{c0} of the unquenched sample is below 60 K then quenching from comparatively low temperature T_q within the range 300 K–450 K results in

a decrease of T_c by ΔT_c; the lower is T_{c0} the larger is ΔT_c. Results of X-ray examination of ceramic samples are also presented, in order to reveal whether the lattice parameters correlate mainly with x or with T_c.

The third section is devoted to theory. It starts with general considerations which are in the background of the theoretical approach to the problem. We assume that T_c is determined by the hole concentration in Cu(2) planes, as it occurs, for instance, in $La_{2-\xi}Sr_\xi CuO_4$. Holes within a Cu(2) plane appear as a result of charge transfer from Cu–O– ... chains. However, the transfer takes place only if chain fragments are long enough. Short chain fragments which contain one, two and, probably, three oxygen atoms do not inject holes. We demonstrate this in the first part of the third section where the microscopical model describing fermionic degrees of freedom is presented. It is applied to compute the free energies of finite chain fragments.

If the oxygen content within a row is fixed then the temperature variations have little effect on the mean length of the chain fragments. However, due to the double-cell structure where only the mean oxygen content is fixed there appears a possibility for more effective rearrangement of these lengths. The second part of the section includes the statistical mechanics of the ensemble of chain fragments. It is supposed to be an acceptable explanation of the alternative oxygen filling of vacancies in the chains. The alternation disappears at the second order phase transition from the double-cell to unit-cell structure. The entropy contribution to the free energy favours shorter fragments in their competition with longer ones, tends to increase the number of short fragments and, therefore, to decrease the carrier concentration in Cu(2) planes and T_c.

The third subsection contains comparison of the experimental results with a rather simple model which reflects partly the properties of chains discussed in subsections 3.1 and 3.2. The model takes into account a competition of two kinds of chain fragments, i.e., very short and long enough. Contrary to the former the latter is assumed to be effective for hole injection into the Cu(2) planes.

The paper ends by a summary where all the main conclusions are collected.

2. Experimental procedure and results

A cylindrical sample of 2 mm in diameter and about 10 mm in length was prepared from YBCO ceramics. X-ray examination did not detect any traces of extraneous phases in this material; its density was 5.6 g/cm^3.

The sample was subjected to vacuum annealing which resulted in a decrease of the oxygen content. The change of the resistance of a bar, made of the same material as the sample in question and placed into a heated vacuum thermal chamber, served to measure the annealing duration. The annealing procedure and experimental conditions have been described in details in ref. [6]. The cooling process from the annealing temperature 450°C to room temperature, which continued approximately 2 h, was supposed to be slow. We did not measure the oxygen stoichiometry directly. Instead, we relied upon the well known dependence of the transition temperature T_c on x [7–9] and determined the state of the sample by its T_c. Since quenching the sample results in a decrease of T_c, we need a definition of the transition temperature unambiguously related to x. It can be determined after slow cooling the sample to room temperature. We denote it by T_{c0}.

After fixing the oxygen content we subjected the sample to another annealing procedure which followed by quenching from temperatures T_q between 50° and 200°C. For this treatment the sample was placed inside a furnace at the normal air pressure. A liquid nitrogen bath was placed just below the furnace and a faint flux of the nitrogen vapor proceeded through the inner tube of the furnace. A sample was processed for some time at fixed temperature T_q (20 min at 200°C and up to 2 h at 50°C) and then thrown into liquid nitrogen from a height of about 10 cm.

The annealing–quenching procedure did not affect the total oxygen content in the sample [4,5]. The shifted T_c value of a quenched sample could be restored by annealing the sample at 100°C for 2 h and further cooling it slowly to room temperature. The T_{c0} value can be also restored by processing a sample for several days at room temperature [10].

After a series of quenching processes and measurements the sample was subjected to new vacuum annealing which resulted in further decline of the ox-

ygen content x. Then a new series of quenching processes was done repeatedly.

In order to determine the temperature of the superconducting transition we performed measurements of the temperature dependence of the real part of the AC-susceptibility $\chi(T)$. The measuring coils were disposed in liquid helium over the external surface of a small overturned dewar while the sample together with a thermometer and a heater were installed inside the dewar. In order to prevent temperature gradients the sample was put inside a sapphire container.

It is well known that the AC-susceptibility of ceramics depends on the amplitude h of the stimulant field. We used an extremely small amplitude, $h=2\times10^{-3}$ Oe, which could certainly provide for χ-independence on h. The measurements were carried out at the frequency 10^5 Hz.

Figure 1 presents typical $\chi(T)$ curves obtained after quenching from different temperatures. The curve labeled by 1 corresponds to the initial state of the sample after vacuum annealing and slow cooling.

$\chi(T)$ curves would have been step-like were it not for scattering of transition temperatures of the grains [11]. We assume that the shift of T_c of a grain depends on its T_{c0} only. If the shift ΔT_c is not a constant but depends on T_{c0} then the curve $\chi(T)$ should change its shape after quenching the sample. However, one can see from fig. 1 that this is not the case, i.e., the quenching procedure results in a parallel shift of the $\chi(T)$ curve, at least, of its middle part $0.2<-4\pi\chi<0.8$. This means that we can neglect the changes of ΔT_c over the width of the T_c distribution and trace the shift along the T-axis at any fixed $\chi(T)$ level. We have chosen the level corresponding to $-4\pi\chi=0.35$.

Figures 2 and 3 present the main results of our measurements of the transition temperature. These are as follows.

(1) A significant shift of T_c to below proceeds from quenching if $T_{c0}<60$ K; the smaller T_{c0}, the larger is its shift; it becomes negligible for $T_{c0}>60$ K.

(2) The shift ΔT_c increases with increasing quenching temperature T_q; this dependence saturates at $T_q\approx200°C$.

So we have confirmed the main results obtained in ref. [4]. The only discrepancy with the results reported in ref. [4] is that the shifts ΔT_c obtained by us are approximately two times smaller. The source

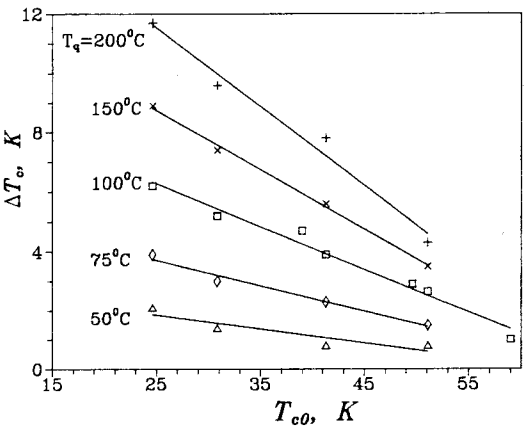

Fig. 2. ΔT_c vs. T_{c0} at different T_qs.

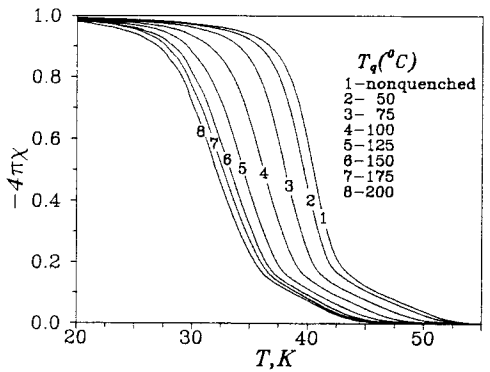

Fig. 1. AC-susceptibility of the sample with a fixed oxygen content after quenching from various temperatures.

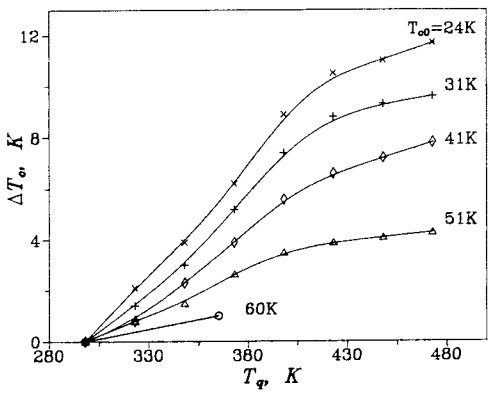

Fig. 3. ΔT_c vs. T_q at different T_{c0}s.

of this discrepancy is unclear. However, it is not due to the difference in the cooling speed. Indeed, the discrepancy still exists at small quenching temperatures when the relaxation time is large enough (note that at room temperature it is of the order of 100 h).

The structure parameter changes as checked by X-ray measurements were for certain rather small. It is not reasonable to compare measurements performed after the various quenching because it has been impossible to restore the mutual positions of the sample and detector with the required precision. Instead, after quenching the sample has been put into the diffractometer at room temperature and a time evolution of the reflection positions has been checked.

The X-ray measurements were carried out on the powder diffractometer D500 (Siemens) with a position sensitive detector. A primary beam monochromator for Cu $K\alpha_1$ line was used. The detector was fixed in the position $2\theta = \text{const} = 46.5°$. So, positions of the sample and detector were fixed both for the whole time of measurements. The time stability of the whole set up was checked by the measurements performed on the unquenched sample. One measurement required 500–2000 sec of counting time. The precise positions of three Bragg peaks (006, 020 and 200) from the selected angle range were resolved by the fitting program. The fitting data are used in fig. 4 to plot the orthorhombic parameter $\beta = (b-a)/(b+a)$ versus time. We ascribe the difference of the final β values observed at different quenching temperatures to inaccuracy of the sample installation. It follows from fig. 4 that a restoration

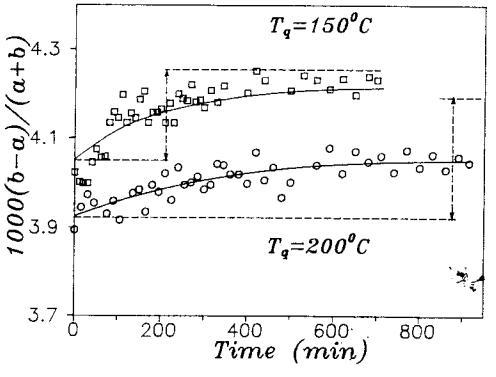

Fig. 4. Orthorhombic parameter drift while annealing the quenched sample. The arrows indicate the drifts calculated at the equilibrium (see explanation in text).

process, resulting in T_c increasing, is accompanied by the parameter β increasing. These changes can be compared with those deduced from the well known data on $T_{c0}(x)$ [7,2] and $\beta(x)$ [9,12]. Excluding x we can get an estimate $\Delta\beta \approx 2.5 \times 10^{-5} \Delta T_c$ for $T_{c0} < 60$ K (ΔT_c measured in K). These values are plotted by vertical arrows in fig. 4 together with the experimental data. The accuracy of this experiment is rather poor and it should be repeated with a single crystal. However, the X-ray measurements give clear evidence that T_c and lattice parameters correlate strongly at the fixed value of x.

The neutron diffraction experiment [13] has demonstrated a similar result, i.e., lattice parameters relaxed after quenching the sample from 500°C. In our opinion, quenchings from 500°C and from 200°C lead to almost the same result because the main changes occur somewhere around 200°C, the temperature close to the ortho-I–ortho-II phase transition (see also section 3.3).

3. Theory

Before analysing the problem quantitatively we briefly remind what kind of elementary transformations happen with oxygen and copper ions within the oxygen deficient Cu(1) layer (see also ref. [14]).

For sufficiently small x, oxygen atoms are supposed to occupy vacant positions, which are situated at horizontal and vertical Cu–Cu bonds, randomly. The elementary fragment Cu^{1+}–O–Cu^{1+} is unstable and under the charge transfer within this group it transforms into the fragment Cu^{2+}–O^{2-}–Cu^{2+}. The transformations of longer chain fragments follow the scheme:

$$Cu^{1+}\text{–O–}Ci^{1+}\text{– ...–O–}Cu^{1+}$$

$$\rightarrow Cu^{2+}\text{–}O^{1-}\text{–}Cu^{2+}\text{– ...–}O^{2-}\text{–}Cu^{2+}\,.$$

It is noteworthy that all copper sites within such a fragment are in the bivalent state (evidence for such a transformation is given in refs. [15] and [16]) whereas there is only one bivalent oxygen; $n-1$ are in the monovalent state, i.e., $n-1$ p-holes exist within a chain fragment. However, sufficiently long chain fragments fail to keep too many oxygen holes within them giving rise to the charge transfer onto Cu(2)

planes. The properties we are interested in here are associated with YBCO in the orthorhombic phase, so we assume that chain fragments forming the chain structure are straight and parallel to each other.

The theory can be accomplished in two steps. First, we need to calculate the internal part of the free energy of the chain fragment consisting of $n+1$ bivalent copper ions, m bivalent oxygen ions and $n-m$ monovalent oxygen ions. Such a fragment is characterized by its ground state energy $\epsilon_0(n, m)$ per one oxygen site and a set of excited states $\{\epsilon(n, m)\}$, contributing the intrachain part

$$\varphi(n, m) = -\frac{T}{n}\ln\left(\sum_{\{\epsilon\}} \exp\left(-n\frac{\epsilon(n, m)}{T}\right)\right) \qquad (1)$$

of the free energy (per one oxygen site again) of such a chain fragment. If all the chain fragments are neutral as compared to the "background" configuration in $YBa_2Cu_3O_6$ (it corresponds to $m=1$ independently on the length of a chain fragment) there is no charge transfer to/from outside. $m-1$ is the number of holes which are injected from a chain fragment onto the Cu(2) plane. It could be even equal to -1. Formally, this means a hole transfer from Cu(2) layer into a neutral chain. In order to control the electrical neutrality of the chain ensemble and holes in Cu(2) layers we redefine the effective fragment energy (per one O site) as follows: $\epsilon(n, m) \to \epsilon(n, m) + ((m-1)/n)\Delta$, where the energy gap ($\Delta$) is associated with a charge transfer onto Cu(2) planes.

Second, deriving the configurational part of the free energy of the chain ensemble we need only the "external" variable characterizing a chain fragment, i.e., its length n, hence, the sum over internal degrees of freedom (m) should be performed. It converts the set $\{\varphi(n, m)\}$ into

$$\varphi(n) = -\frac{T}{n}\ln\left(\sum_{m=0}^{n} \exp\left(-\frac{n\varphi(n,m) + (m-1)\Delta}{T}\right)\right). \qquad (2)$$

In order to calculate the abovementioned chain characteristics like $\epsilon_0(n, m)$, $\epsilon(n, m)$, $\varphi(n, m)$ and $\varphi(n)$ we need a microscopical model which is discussed in the following subsection.

3.1. Microscopic description of chain fragments

Among different candidates to describe the fermionic degrees of freedom we prefer the Kondo-like version [14] of the Emery model [17]. It can be derived in the second order of the perturbation theory. In the framework of such Kondo-reduced Emery model oxygen holes are responsible for the Kondo-like charge transfer within a chain fragment. It is accompanied by scattering of two spins, i.e., of the mobile oxygen hole and of the practically localized copper hole. Besides such a "kinetic" energy term, the antiferromagnetic Heisenberg-like spin exchange of neighbouring oxygen and copper holes is taken into account as well as the intrachain Coulomb interaction. Because of the high polarizability of oxygen the latter decreases with distance rapidly, so we keep its short-ranged part, i.e., the nearest Cu–O and O–O interactions.

We present the total Hamiltonian in the following form:

$$H = H_K + H_C . \qquad (3)$$

Its Kondo-like part is

$$H_K = t_k \sum_R \left(c^\dagger_{R-a/2,\alpha} Z^{\beta\alpha}_R c_{R+a/2,\beta} + \text{h.c.}\right) + J_k \sum_{r=R\pm a/2} Z^{\alpha\beta}_r Z^{\beta\alpha}_R , \qquad (4)$$

where R and $R \pm a/2$ label the copper and oxygen sites, respectively. $c^\dagger_r$ (c_r) creates (annihilates) the mobile hole on the oxygen site r. $Z^{\beta\alpha}$ permutes the hole spin projection $\alpha \to \beta$.

The second term in the Hamiltonian (3) is the Coulomb interaction

$$H_C = U_{pd} \sum_{\langle R,r\rangle} \rho_R \rho_r + \tfrac{1}{2} U_{pp} \sum_{\langle r,r'\rangle} \rho_r \rho_{r'} , \qquad (5)$$

where $\Sigma_{\langle \ldots \rangle}$ runs over either the nearest Cu and O (R and r) sites or the nearest O sites (r and r'). ρ is the on-site electrical charge as compared to the stoichiometrical charge distribution in $YBa_2Cu_3O_6$, i.e., within a chain fragment $\rho_R = 1$ and $\rho_r = -2$ or -1. The contribution of the first term in the RHS of eq. (5) to the energy per one oxygen site can be easily evaluated as $-2U_{pd}(1+m/n)$.

Before exhibiting the numerical results we briefly discuss the role of the terms entering the Hamilto-

nian H and their contribution to the energy. The Kondo-like exchange takes the minimal value when $m=0$. The Kondo-like hopping term favours the proportion $m \approx n/2$ like in typical tight-binding strongly correlated fermion systems. The part $(m/n)\Delta$ of the charge-transfer energy can be included in the U_{pd}-term, renormalizing it. Hence, only the contribution $-(1/n)\Delta$ should be considered as independent. Evidently, this U_{pd}-term favours O^{2-} states whereas U_{pp} tends to minimize their amount.

The plot of the ground state energy versus m/n is shown in fig. 5(a) and (b). $\epsilon_0(n, m)$ has been calculated in the framework of the Lanczos algorithm (see for instance ref. [18]), nowadays it is often applied to the finite strongly correlated systems. The solid curves in figs. 5 are splines of the data obtained for the chain fragment consisting of nine copper and eight oxygen ions. The energy parameters t_k and J_k were taken from the numerical calculations reported by Sawatzky [19]. The other parameters were selected in order to satisfy the estimate of the hole concentration in Cu(2) planes. This amount is supposed to be approximately the same for the $YBa_2Cu_3O_7$ and for the $La_{2-\xi}Sr_\xi CuO_4$ compound. The optimal ξ is about 0.2 whereas the optimal $x \approx 1$. The fraction of oxygen holes leaving long Cu–O– ... fragments is equal approximately to m/n. Multiplying it by $\frac{1}{2}x$ we should get the product equal approximately to ξ. The factor $\frac{1}{2}$ reflects the structural element of YBCO which contains two Cu(2) planes per one Cu(1) plane. Hence, m/n can be evaluated as ≈ 0.4–0.5.

The essential conclusion follows from figs. 5: short chain fragments cannot inject the holes onto Cu(2) planes. There is no question in the case $n=1$. A neutral chain fragment ($n=2$, $m=1$) defeats two other candidates with $n=2$. A chain fragment ($n=3$, $m=2$) charged negatively is also unfavourable energetically except for the minimum of the ground state energy curve in figs. 5 that is situated rather close to $m/n \approx \frac{2}{3}$. Most likely, longer chain fragments ($n \geqslant 4$) contribute the charge transfer: the set of energetically favourable fragments starts with $n=4$, $m=2$. Note that the term Δ/n results only in an additive shift of the plot.

The situation illustrated in fig. 5(a) is favourable for chain fragments with $m/n \approx 0.5$. The finite chain fragments with $n=3$ and $m=1$, 2 and, certainly, the shortest ones with $n=1$, $m=1$ should also be included into the set of competing structural elements. On the contrary, fig. 5(b) demonstrates the more general case when Cu–O–Cu appears to be energetically unfavourable. Hence, it is necessary to keep in mind the model with fragments of the length $n=2$ as the shortest competing elements.

Recall that the content of subsection 3.1 is based on the ideas developed in ref. [14].

3.2. Free energy of the chain ensemble: configurational contribution

Here we derive the equations which could be acceptable for the description of orthorhombic phases including the possibility for a double-cell structure.

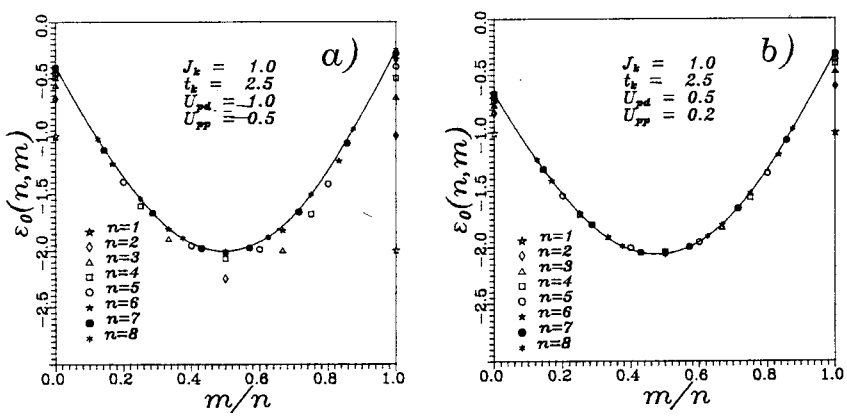

Fig. 5. The ground state energy of a chain fragment vs. m/n (see explanation in text).

We suppose, that the ortho-II phase with the oxygen content altering from chain to chain in the Cu(1) planes can be formed due to the Coulomb interaction in the neighbouring rows. We accept the simplest form of the repulsive interaction proportional to the concentration of oxygen ions in the nearest rows, i.e., oxygen is supposed to be distributed homogeneously within a whole chain (see below, eq. (6)).

In order to derive the partition function of the ensemble of chains with a preferable orientation we introduce the following notation.

$N_j^{(\alpha)}$ and $x_j^{(\alpha)}$ are the whole number and concentration of chain fragments of length j either within an oxygen-rich chain or within an oxygen-poor chain ($\alpha=1,2$). Evidently, any chain fragment Cu–O– ...–Cu is surrounded with Cu–Cu bonds free of oxygen ions. One of these bonds, for instance, from the RHS can be joined in the chain fragment. Hence, a chain fragment consists of a chain Cu–O– ...–Cu plus a neighbouring oxygen vacancy. According to this definition we consider also "empty" chain fragments. An example of such a fragment could be two oxygen vacancies following one by another: the first is included into a chain fragment of nonzero length, the second corresponds to $j=0$. According to this definition

$$\sum_{n=0}(n+1)x_n^{(\alpha)}=1\,,$$

besides

$$\sum_{n=0} n(x_n^{(1)}+x_n^{(2)})=2x\,.$$

From the two equations above we obtain:

$$\sum_{n=0}(x_n^{(1)}+x_n^{(2)})=2-2x\,.$$

The Lagrange multipliers corresponding to the constraints imposed on the concentration of different chain fragments play the roles of chemical potentials denoted below as μ_1, μ_2 and μ_0. We denote also

$$S_\alpha=\sum_{n=0} x_n^{(\alpha)}\,.$$

A complete number of different configurations of the chain fragments of any possible length, from 0 to infinity, has a form usual for a mixture of ideal gases:

$$\frac{(N_0+N_1+\ldots+N_m+\ldots)!}{N_0!N_1!\ldots N_m!\ldots}\,.$$

After straightforward transformations we get the partition function per one chain:

$$\begin{aligned}\mathscr{Z}=\sum\exp\frac{N}{2}\{&S_1\ln S_1+S_2\ln S_2-x_0^{(1)}\ln x_0^{(1)}\\&-x_0^{(2)}\ln x_0^{(2)}-\ldots-x_n^{(1)}\ln x_n^{(1)}-x_n^{(2)}\ln x_n^{(2)}-\ldots\}\\&\times\exp\left(-\frac{N\sum_{n=1}n\varphi(n)(x_n^{(1)}+x_n^{(2)})}{2T}\right)\\&\times\exp\left(-N\frac{V}{T}S_1S_2\right)\\&\times\exp\left(\frac{N\sum_{n=0}(n+1)(\mu_1x_n^{(1)}+\mu_2x_n^{(2)})}{2T}\right)\\&\times\exp\left(-\frac{N\mu_0\sum_{n=0}(x_n^{(1)}+x_n^{(2)})}{2T}\right),\end{aligned}\qquad(6)$$

where N is the total number of Cu(O) sites within a chain. The V-term accounts for the Coulomb interchain repulsion in the simplest form of a density–density interaction.

According to the conventional recipes of statistical physics we maximize the exponential arguments in eq. (6) over the set $\{x_n^{(\alpha)}\}$ by using the Lagrange multipliers:

$$\begin{aligned}x_n^{(1)}&=S_1\exp\frac{-n(\varphi(n)-\mu_1)+(\mu_1-\mu_0)-2VS_2}{T}\,,\\x_n^{(2)}&=S_2\exp\frac{-n(\varphi(n)-\mu_2)+(\mu_2-\mu_0)-2VS_1}{T}\,.\end{aligned}\qquad(7)$$

The Lagrange multipliers μ_0, μ_1, μ_2, together with the quantities S_1 and S_2 depend on microscopical parameters and temperature as follows:

$$S_1+S_2=2-2x\,,\qquad(8)$$

$$\exp-\frac{\mu_1-\mu_0-2VS_2}{T}=\sum_{n=0}\exp-\frac{n(\varphi(n)-\mu_1)}{T}\,,\qquad(9)$$

$$\exp-\frac{\mu_2-\mu_0-2VS_1}{T}=\sum_{n=0}\exp-\frac{n(\varphi(n)-\mu_2)}{T}\,,\qquad(10)$$

$$\exp -\frac{\mu_1-\mu_0-2VS_2}{T}$$

$$=S_1\sum_{n=0}(n+1)\exp-\frac{n(\varphi(n)-\mu_1)}{T}, \qquad (11)$$

$$\exp -\frac{\mu_2-\mu_0-2VS_1}{T}$$

$$=S_2\sum_{n=0}(n+1)\exp-\frac{n(\varphi(n)-\mu_2)}{T}. \qquad (12)$$

We introduce the notation

$$z_\alpha=\exp\frac{\mu_\alpha-\varphi(1)}{T},$$

$$\gamma_n=\exp\frac{n(\varphi(1)-\varphi(n))}{T}.$$

Dividing eq. (11) and eq. (12) over eq. (9) and eq. (10), respectively, we get

$$S_\alpha=\frac{1+\gamma_1 z_\alpha+\gamma_2 z_\alpha^2+\ldots+\gamma_n z_\alpha^n+\ldots}{1+2\gamma_1 z_\alpha+3\gamma_2 z_\alpha^2+\ldots+(n+1)\gamma_n z_\alpha^n+\ldots}. \qquad (13)$$

The analogous procedure applied to eqs. (10) and (9) results in

$$G(z_1)=G(z_2), \qquad (14)$$

where

$$G(z)=\frac{2VS_1}{T}+\ln z+\ln(1+\gamma_1 z+\gamma_2 z^2+\ldots). \qquad (15)$$

The last two terms in the RHS of eq. (15) are monotonic functions of z and dominate in the asymptotic behaviour of the function $G(z)$ at $z\to 0$ and at $z\to\infty$. Due to the monotonic decrease of $S(z)$ with z increasing the first term in the RHS of eq. (15) may result in a nonmonotonic dependence of $G(z)$ on z at sufficiently low temperatures.

The formal expression of the free energy per lattice site takes the form

$$f=\tfrac{1}{2}(\mu_1+\mu_2)-(1-x)\mu_0-VS_1S_2.$$

Omitting irrelevant constants and expressing f as a function of z_α, we obtain

$$f=\frac{T}{2}\Big\{-\frac{2V}{T}S_1S_2+x(\ln z_1+\ln z_2)-(1-x)(\ln(1+\gamma_1 z_1+\gamma_2 z_1^2+\ldots)+\ln(1+\gamma_1 z_2+\gamma_2 z_2^2+\ldots)\Big\}. \qquad (16)$$

The equilibrium concentration of chain fragments derived from eqs. (7,9,10) takes the following form:

$$x_n^{(\alpha)}=\frac{\gamma_n z_\alpha^n}{1+2\gamma_1 z_\alpha+3\gamma_2 z_\alpha^2+\ldots+(n+1)\gamma_n z_\alpha^n+\ldots}. \qquad (17)$$

Let assume the microscopic parameters, i.e., the set of $\{\gamma_n\}$s and V to be known. Then solving eq. (14) we find, in general, an ambiguous dependence $z_2(z_1)$, $z_2\geqslant z_1$. After substitution of z_α into eqs. (13) we must solve eq. (8). The calculation procedure is completed by checking the free energy defined by eq. (16). The problem is rather complicated to be solved analytically even after significant simplifications like those made in subsection 3.3.

The general numerical analysis of the problem is straightforward and below we describe a regular approach to perform it.1 The calculations are based on the similarity of the intrinsic free energy curve and the ground state energy one versus m/n. Actually, for finite chains the excitation energies are usually much larger than T. For long chains a contribution of thermal excitations to the free energy is proportional to T^2/ϵ_f and is rather small, because, in general, $\epsilon_f\sim t_k\gg T$. It would be possible to perform the Gauss-like summation over m in eq. (2) for sufficiently long chain fragments. This procedure seems to be well-defined for fragments with $n\geqslant 5$. We need only to do a formal expansion of $\varphi(n, m)$ in the $n\to\infty$ limit around its minimum corresponding to $m/n=\eta$ and extrapolate such an expansion to finite ns:

$$\varphi(n, m)=\psi_0(\eta)+\frac{1}{2}\psi_2\left(\frac{m}{n}-\eta\right)^2+\frac{1}{n}\psi_1(\eta). \qquad (18)$$

The further summation over n seems to transform the set of sufficiently long chain fragments into some effective fragment with renormalized intrinsic parameters, including free energy, length, hole filling, etc. Joining the contribution of chain fragments with $n\leqslant 5$ we get the complete prerequisite for solving the

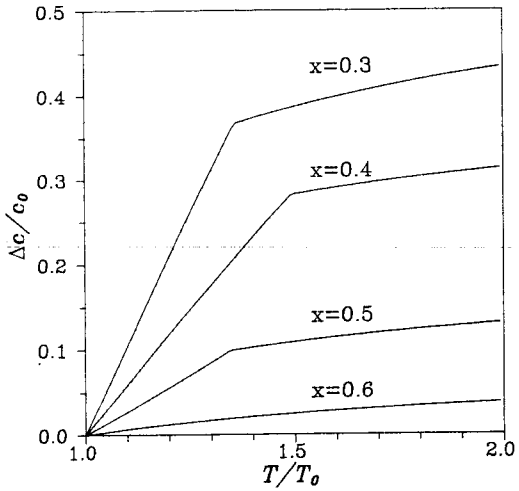

Fig. 6. Theoretical calculations of the hole concentration vs. temperature at various oxygen contents.

system of equations describing the behaviour of the orthorhombic phase. This project will be realized in further publications. In this paper we restrict ourselves to a simple model where a competition of two kinds of fragments is taken into account.

3.3. Competition of chain fragments; a simple model description

Let us suppose that energetically favourable fragments are the shortest Cu–O–Cu chains ("monomers" with $n=1$) and 4-mers. In other words all γ_n except γ_4 are supposed to be negligible. Monomers are neutral whereas the electrical charge of a 4-mer is supposed to be -1, i.e., it supplies a Cu(2) plane with one hole.

The energy parameters required to solve the problem are V and $\varphi(1)-\varphi(4)$; both are relevant for the ortho-I–ortho-II transition temperature T_{1-2} evaluation. It is essential that the interchain Coulomb repulsion screened partially cannot exceed 0.1–0.2 eV, otherwise T_{1-2} appears to be unreasonably high. The analogous estimate should be valid for the energy difference $4(\varphi(1)-\varphi(4))$, otherwise existence of the insulator phase corresponding to $x<0.4$ would be difficult to interpret.

In fig. 6 the results of numerical calculations are shown for $V=2.5$ and $4(\varphi(1)-\varphi(4))=2$. Both values are given in units of some temperature T_0, defined more or less arbitrary, except it should be higher than the temperature of oxygen migration T_m.

According to one of our basic assumptions made in section 1 T_c depends on the carrier concentration $c(x, T_q)$ in Cu(2) planes. Then

$$T_{c0}=T_c(c(x, T_0))$$

and

$$\begin{aligned}\Delta T_c &= T_{c0}-T_c \\ &= T_c(c(x, T_0))-T_c(c(x, T_q)) \\ &\approx \frac{dT_c}{dc}\,(c(x, T_0)-c(x, T_q))\,. \end{aligned} \tag{19}$$

Hence, measurements of ΔT_c and $\Delta c(x, T_q)=c(x, T_q)-c(x, T_0)$ are equivalent for a wide range of T_{c0} up to 50 K where $dT_c/dc\approx$ const.

In fig. 6 the curves $\Delta c(x, T_q)$ exhibit a kink associated with the ortho-II–ortho-I phase transition. To the left of the kink, in ortho-II phase, the temperature increase provokes oxygen rearrangement between the rows. This results in a steep slope of the function Δc. To the right of the kink, in ortho-I phase, the rows are equivalent, the concentration of oxygen vacancies for each row

$$S_1=S_2=1-x$$

does not depend on temperature. Accordingly, the slope becomes slight because at the fixed number of vacancies the distribution of fragments over their lengths varies slightly with temperature.

Comparing fig. 6 and fig. 3 we identify T_0 with room temperature and get the ortho-II–ortho-I transition temperature $T_{1-2}\approx 150$°C. This correlates with the estimate of T_{1-2} obtained in ref. [6] from the resistance versus temperature data in YBCO ceramics. Similarities between the curves in figs. 3 and 6 support the choice of parameters in our simplified model and the model itself.

4. Concluding remarks

Let us bring all the assumptions and results together to form a self-consistent pattern. Transport properties of YBCO materials and their superconducting transition temperatures are determined by the carrier concentration in the Cu(2) planes. The

carriers appear due to the charge transfer from Cu–O– ... chain fragments to the Cu(1) planes. In sufficiently long fragments ($n \geqslant 4$) the fraction of oxygen ions, which supply Cu(2) planes with holes, ranges from ≈ 0.4 to ≈ 0.5. Short fragments ($n = 1$, 2, 3) do not inject holes, hence, do not contribute to the transport properties of the material.

The distribution of fragments over their lengths depends on x and on the type of orthorhombic phase. At moderate temperatures and x near 0.5 a majority of oxygen ions are collected in oxygen-rich rows and fragments within them are long enough. With x increasing additional oxygen atoms are accommodated by oxygen-poor rows. As far as the oxygen concentration in oxygen-poor rows remains small the atoms are mainly incorporated into short fragments, hence, do not contribute to the hole concentration in the Cu(2) planes. This brings out the plateau-like behaviour in $T_c(x)$.

The ortho-II–ortho-I phase transition arises from the increase of temperature. In the ortho-I phase all chains are equally filled with oxygen. When its concentration x is large enough (for instance, $x \approx 0.6$–0.7) the fraction of short fragments is small. The smaller is x, the larger is the fraction of short fragments resulting in a decrease of carrier concentration c in the Cu(2) planes. After quenching the sample from T_q the distribution of chain fragments over their lengths reflects the equilibrium at the quenching temperature. It concern also c bringing about the ΔT_c shift.

The change of lattice parameters shown in fig. 4 (see also ref. [13]) confirms indirectly the charge transfer model discussed above. A change of hole concentration means a charge redistribution inside the unit cell. This alters its size. If ΔT_c were caused by changes of magnetic states of chain fragments it would not be accompanied by variation of lattice parameters.

An independent check of the suggested model can be performed by measuring the temperature T_{1-2} of the ortho-I–ortho-II phase transition.

Acknowledgements

GU wishes to thank J. Ranninger, J. Rossat-Mignod and A. Fontaine for very fruitful discussions.

References

[1] C. Chaillout, M.A. Alario-Franco, J.J. Capponi, J. Chenavas, P. Strobel and M. Marezio, Solid State Commun. 65 (1988) 283.
[2] R. Beyers, B.T. Ahn, G. Gorman, V.Y. Lee, S.S.P. Parkin, M.L. Ramirez, K.P. Roche, J.E. Vazquez, T.M. Gur and R.A. Huggins, Nature 340 (1989) 619.
[3] J.P. Locquet, J. Vanacken, B. Wuyts, Y. Bruynseraede and I.K. Schuller, Europhys. Lett. 10 (1989) 365.
[4] H. Claus, S. Yang, A.P. Paulikas, J.W. Downey and B.W. Veal, Physica C 171 (1990) 205.
[5] K.V. Vandervoort, G.W. Crabtree, Y. Fang, S. Yang, H. Claus and J.W. Downey, Phys. Rev. B 43 (1991) 3688.
[6] V.F. Gantmakher and D.V. Shovkun, JETP Lett. 51 (1990) 471.
[7] R.J. Cava, B. Batlogg, C.H. Chen, E.A. Rietman, S.M. Zahurak and D. Werder, Phys. Rev. B 36 (1987) 5719.
[8] J. Rossat-Mignod, P. Burlet, M.J. Jurgens, C. Vettier, L.P. Regnault, J.Y. Henry, C. Ayache, L. Forro, H. Noel, M. Potel, P. Gougeon and J.C. Levet, J. Phys. (Paris) C 8 (1988) 2119.
[9] R.J. Cava, A.M. Hewat, E.A. Hewat, B. Batlogg, M. Marezio, K.M. Rabe, J.J. Krajewski, W.F. Peck Jr. and L.W. Rupp Jr., Physica C 165 (1990) 419.
[10] B.W. Veal, H. You, A.P. Paulikas, H. Chi, Y. Fang and J.W. Dowey, Phys. Rev. B 42 (1990) 4770.
[11] V.F. Gantmakher, A.M. Neminsky and D.V. Shovkun, Physica C 177 (1991) 469.
[12] J.D. Jorgensen, B.W. Veal, A.P. Paulikas, L.J. Nowicki, G.W. Crabtree, H. Claus and W.K. Kwok, Phys. Rev. B 41 (1990) 1863.
[13] J.D. Jorgensen, S. Pei, P. Lightfoot, A.P. Paulikas and B.W. Veal, Physica C 167 (1990) 571.
[14] G. Uimin and J. Rossat-Mognod, to be published.
[15] J.M. Tranquada, S.M. Heald, A.R. Moodenbaugh and Youwen Xu, Phys. Rev. B 38 (1988) 8893.
[16] H. Tolentino, A. Fontaine, F. Baudelet, T. Gourieux, G. Krill, J.Y. Henry and J. Rossat-Mignod, to be published.
[17] V. Emery, Phys. Rev. Lett. 58 (1987) 2794.
[18] E.R. Gagliano, E. Dagotto, A. Moreo and F.C. Alcaraz, Phys. Rev. B 34 (1986) 1677.
[19] G.A. Sawatzky, Int. J. Mod. Phys. B 1 (1988) 243.